*Limnol. Oceanogr.*, 43(6), 1998, 1133–1146


# Resource competition in a discrete environment: Why are plankton distributions paradoxical?

*David A. Siegel*
Institute for Computational Earth System Science, Department of Geography, and Donald Bren School of Environmental Science and Management, University of California, Santa Barbara, California 93106-3060

*Abstract*

For nearly all natural waters, planktonic organisms will be distributed discretely in the fluid mechanical sense. This means that the dynamics of planktonic ecosystems occur among discrete particles, not continuous scalar fields. This idea was first suggested by Hurlburt (1990) as an explanation for the paradox of the plankton. However, the discrete nature of organism distributions has many important implications for the interpretation and modeling of planktonic ecosystems. In particular, mass conservation relationship approaches to the modeling of planktonic populations (i.e., resource competititon and its result, competitive exclusion) will not be valid for all natural conditions. A microscale model of competition among individual phytoplankton cells was used to investigate the role of discreteness on phytoplankton competitition for a single, limiting nutrient substrate. This scaling analysis demonstrates that rates of competitition should increase with cellular abundance and phytoplankton size. For a typical eutrophic planktonic ecosystem (relatively large cell abundances and cell sizes), resource competitition among individual phytoplankters appears to be likely. However, for oligotrophic conditions (low cell abundances and small cells), rates of competitive displacement should be greatly reduced. The microscale competition model does not predict that the final outcome of competition will differ from resource competition theory when evaluated over thousands of division cycles. However the time required for this outcome to occur may be so long that other processes, such as episodic nutrient inputs, imposed diel cycles, and specialization of the grazer assemblage, are likely to have a dominant role in determining the species composition of an oligotrophic phytoplankton community. This seeming violation of the principle of competitive exclusion occurs because nutrient competition in oligotrophic environments is governed by interactions among discrete individuals rather than entire populations. Discreteness in plankton distributions also creates an ecological subgrid scale (SGS) problem that must be solved as part of most mathematical descriptions of plankton population dynamics. Approaches towards solution of the ecological SGS problem are suggested; however, a great deal of theoretical and experimental work remains.

A microscopic examination of a natural water sample often reveals a great diversity of planktonic organisms even in the open ocean, where it is presumed that low nutrient concentrations will limit phytoplankton production. Assuming that phytoplankton growth is limited by the supply of a limiting nutrient, the one species that is best able to utilize this limiting resource will become numerically dominant; this is simply an application of the principle of competitive exclusion (e.g., Tilman 1982). However, diverse assemblages of phytoplankton are generally observed in natural waters, especially in oligotrophic regions, implying that many phytoplankton species can successfully coexist while competing for at most a few limiting nutrients. Hutchinson (1961) referred to this apparent exception to the principle of competitive exclusion as the paradox of the plankton.

Laboratory experiments have provided important information concerning the rates at which individual phytoplankton species compete for a limiting nutrient (e.g., Tilman 1977; Tilman et al. 1981; Sommer 1983, 1985). For example, Tilman et al. (1981) investigated competition between two freshwater diatoms (*Asterionella formosa* and *Synedra ulna*) for a limiting silicate resource in a semicontinuous batch culture (Fig. 1). Specific growth rates for *S. ulna* are faster than those for *A. formosa* at all concentrations of the limiting substrate, indicating that *S. ulna* should always outcompete *A. formosa* for silicate (Fig. 1a). As expected, when the two diatoms compete for silicate, *S. ulna* dominates the final assemblage independent of the initial abundances of the competitors (Figs. 1d–f).

These laboratory results have also been successfully modeled using resource-based competititon theory (e.g., Tilman 1982; Tilman et al. 1982; Sommer 1989). Resource-based competititon theories predict temporal changes in the concentrations of a limiting resource (here, silicon) for each of the relevant pools that may be used to forecast changes in the composition of an assemblage. Assuming Michaelis-Menten uptake kinetics and a constant density-dependent mortality rate ($m$) hold, the competititon equations for the present example (Fig. 1) are

$$\frac{dC_{Af}}{dt} = \frac{V_{mAf}S}{K_{Af} + S}C_{Af} - mC_{Af} \quad (1a)$$

$$\frac{dC_{Su}}{dt} = \frac{V_{mSu}S}{K_{Su} + S}C_{Su} - mC_{Su} \quad (1b)$$

$$\frac{dS}{dt} = -\frac{dC_{Af}}{dt} - \frac{dC_{Su}}{dt}, \quad (1c)$$

*Acknowledgments*

Mark Brzezinski made many important contributions to the interpretations presented and to my training as an amateur phytoplankton ecologist; both of which are gratefully acknowledged. Discussions, comments, and/or reviews from Tony Michaels, Julie Siegel, Scott Doney, Peter Franks, Libe Washburn, David Tilman, Margaret O'Brien, and the anonymous reviewers were all instrumental in development of this work. I thank Julie Siegel for her patience through the many revisions of this manuscript.

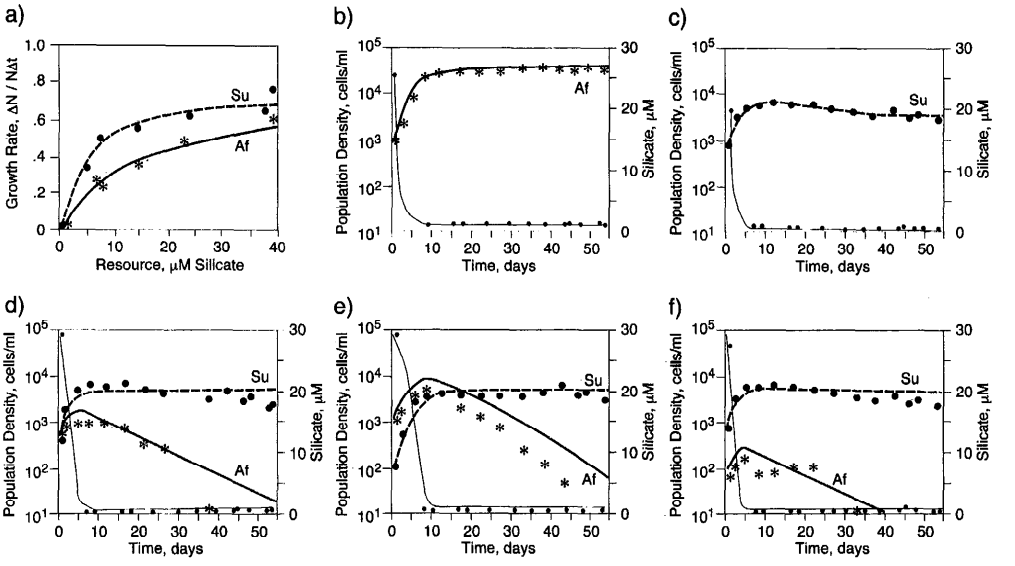


Fig. 1. The results of a silicate competition experiment between two freshwater diatoms, *Asterionella formosa* (Af) and *Synedra ulna* (Su). *A. formosa* forms long spindle-shaped chains of cells where each cell is 40–130 μm long and 1–2 μm across. *S. ulna* is a narrow pennate species with a length of 50–350 μm and a width of 4–9 μm. Results from the semicontinuous batch culture experiments are shown as the symbols, and the results of the resource competition model (Eq. 1) are shown as the solid lines. The dilution (mortality) rate of the culture is 0.11 $d^{-1}$ and the vessel temperature is 24°C. a) The dependence of the specific growth rate of each species on the silicate concentration from separate short-term batch culture experiments. Time-course changes in abundances for monocultures of *A. formosa* (b) and *S. ulna* (c) with silicate concentrations. Final silicate values are higher for *A. formosa* (1.0 μM $SiO_2$) than for *S. ulna* (0.4 μM $SiO_2$), indicating that *S. ulna* will be the better competitor for silicate. Abundance changes of *A. formosa* and *S. ulna* (d–f) because of resource competition for three different starting abundances for the two species. As expected, *S. ulna* will dominate the final assemblage when both diatom species are competing for the limiting silicate resource. Figure is adapted from Tilman (1982).

where $S$ is the concentration of the limiting silicate substract, $C_{Af}$ and $C_{Su}$ are the concentrations of silicone in *A. formosa* and *S. ulna,* respectively, $V_{mAf}$ and $V_{mSu}$ are their maximum specific uptake rates, and $K_{Af}$ and $K_{Su}$ are their half-saturation constants, defined as the silicate concentration where the specific uptake rates is one-half of $V_{mAf}$ and $V_{mSu}$. The predictions made by this numerical analogy to the culture experiment are nearly identical to the experimental results (see the lines in Fig. 1; where abundance is calculated using mean cell quotas). This comparison illustrates that resource-based competition models work well for predicting the results of these laboratory based experiments. However, natural communities are often characterized by coexistence of many phytoplankton species. This is Hutchinson's (1961) paradox.

Many hypotheses have been forwarded to explain the cause of the paradox of the plankton. Some have suggested that the large observed phytoplankton diversity is a consequence of simultaneous limitation by many resources (e.g., Peterson 1975; Tilman 1977, 1982). Although this multisource limitation is possible, it is unlikely because there are often more algal species observed than possible limiting nutrients (e.g., Hutchinson 1961). It has been suggested that coexistence may be the result of the infinite number of possible ratios of resource concentrations that can occur in evolving natural system (e.g., Tilman 1982). Others have postulated that the extensive phytoplankton diversity may be created by specialization of the grazer community (Paine 1966). Photocycles can affect nutrient uptake rates and thereby be a factor leading to coexistence (Brzezinski and Nelson 1988). Temporal variations in the external supply of nutrients may also influence rates of exclusive displacements (e.g., Hutchinson 1961; Sommer 1984, 1985). Although a high degree of temporal stochasticity in the new nutrient supply exists for all natural waters, it remains unlikely that the necessary conditions occur for all times and all environments. Others still have suggested that the inherent patchiness in phytoplankton distributions enables competitive displacements to occur for individual patches (Richerson et al. 1970). In effect, Richerson and his colleagues suggest that each water parcel comprises an autonomous and distinct environment in which the plankton reach their temporal equilibrium. There have also been suggestions that the random sorting of phytoplankton cells by turbulent eddies can promote coexistence (Kemp and Mitsch 1979).

Of the wide variety of hypotheses presented attempting to explain Hutchinson's paradox, each has some merit and some defect. It is not the primary intent of this contribution to develop another explanation for the paradox of the plankton but rather to investigate the role of microscale interactions within a natural phytoplankton community and their effect on rates of resource competition. I demonstrate here that nearly all natural phytoplankton populations are distrib-

uted discretely in the fluid mechanical sense. Hence, the resource-based competititon expressions (Eq. 1a–c), which are essentially conservation of mass approaches for describing phytoplankton dynamics, will be valid only rarely for natural waters. Scaling analyses are used to develop a discrete-based microscale model of phytoplankton competition. These results indicate that phytoplankton cells are nearly always too far apart from one another to directly interact with their neighbors on an instantaneous basis. Only for large phytoplankton cells at high abundances will adjacent cells begin to interact with their neighbors. In particular for oligotrophic environments, discreteness will reduce rates of species interaction from estimates based upon vital rates alone. Discreteness may not affect the final outcome of competititon when assessed over many generations. However, it is likely that other processes, such as those listed above, will have the dominant role in determining phytoplankton community composition in oligotrophic waters. I also discuss how the effects of discreteness need to be addressed for the modeling of planktonic ecosystem dynamics.

## Spatial scales for distributions of organisms

Implicit in the mathematical statement of resource conservation is the assumption that changes in plankton population density can be modeled in terms of the numerical abundance of planktonic organisms within a given volume. This volume must be large enough so that determinations of organism abundance (number per unit volume) are statistically stable. The uncertainty in a mean estimate decreases with the square root of the number of individual events counted, based upon Gaussian statistics. Hence, statistically stable estimates of plankton abundance, $P_i(t)$, will occur when a large number of individuals are counted or, equivalently, when a large enough water parcel, $V_p$, is considered. Mathematically, the calculation of plankton number density can be expressed as

$$P_i(t) = \frac{1}{V_p} \int_{V_p} \sum_{j}^{N_i} \delta(\vec{x}_{ij}(t) - \vec{x}')\, d\vec{x}', \qquad (2)$$

where $\vec{x}_{ij}(t)$ denotes the spatial location of the $j$th cells of the $i$th species, $\delta(\vec{x} - \vec{x}_o)$ is the Dirac-delta function, which is equal to zero except at location $\vec{x}_o$ when it is equal to 1, and the summation is over the total number of cells ($N_i$) of species $i$ in the volume $V_p$. In essence, Eq. 2 "counts" the number of organisms within the volume $V_p$. The linear length scale that characterizes this volume, $V_p$, I denote as the parcel scale, $L_p$.

A conceptual depiction of the relationship between $L_p$ and other relevant scales that characterize the spatial distribution of a population of organisms is shown in Fig. 2. Most notable is the length scale, which characterizes the size of the organisms, the equivalent spherical volume diameter ($D_{\text{cell}}$), and the mean separation scale between adjacent organisms, $\lambda$. The mean separation scale, equivalent to the mean free path, is defined here as the linear dimension of the cubic volume occupied by a single phytoplankter and is equal to $P^{-1/3}$, where $P$ is the plankton abundance. For a random (Poisson) distribution of particles, the expectation value for $\lambda$ is

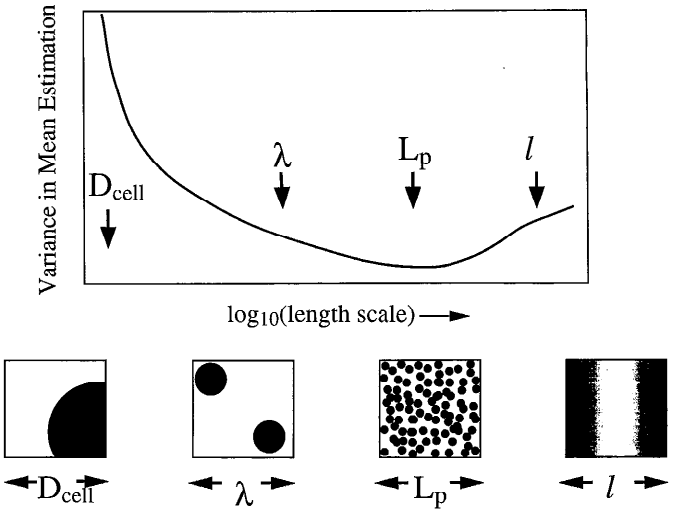


Fig. 2. A comparison of the uncertainty in volume averaged estimates of plankton abundances as a function of length scale. Length scales indicated are the cell's diameter ($D_{\text{cell}}$), the mean separation scale between organisms ($\lambda$), the parcel scale ($L_p$), and the macrolength scale over which the organism's population density varies due to biological and physical processes ($l$). Our depiction of the uncertainty levels in mean abundance estimation is only an educated guess. The lower panel illustrates conceptually the number of particles sampled when viewed at the given length scale.

$0.55P^{-1/3}$ (Rothschild 1992). This small difference in the definition of mean separation scale is unimportant in the order-of-magnitude scaling analyses explored here. Many organisms will be counted over a scale $L_p$, whereas very few will be found over a scale $\lambda$ (Fig. 2). Only rarely will a plankter be encountered when examined at a scale of the size of the organism, $D_{\text{cell}}$. The scale over which the organism's abundance varies is denoted as $l$, and this scale represents the tens of centimeters to thousands of kilometers scales over which we want to assess and predict changes in plankton population density.

Variations in organism abundance viewed on scales larger than $L_p$ will appear continuous, whereas when spatial population densities are viewed on scales smaller than $L_p$ they will appear discrete. This distinction can be understood using the analogy of a microscope. If one were to examine plankton distributions with a microscope that was able to focus only on spatial scales $\geq L_p$, the distribution of organisms would appear as a great blur. If this microscope focuses on objects much smaller than $L_p$, individual organisms will be discerned. The lower four panels of Fig. 2 represent this microscope analogy.

Critical to application of resource competititon expressions or other similar population systems is the determination of the parcel scale $L_p$. An estimate for the parcel scale may be made by determining the smallest volume that contains a sufficient number of cells to allow an accurate determination of cell abundance. As a first approximation, the size of $L_p$ can be determined by evaluating the volume occupied by 400 organisms. The choice of 400 particles is based upon counting statistics, where accurate abundance estimates come from counting large numbers of cells (~1%

Table 1. Largest observed phytoplankton abundances from a variety of aquatic environments. Only the largest concentrations are shown; 1 $ml^{-1}$ is equal to $10^6$ $m^{-3}$. The maximum abundances shown were from a survey of more than 50 studies from a varicty of aquatic ecosystems. For contrast, data from the laboratory simulation shown in Fig. 1 are included.

| Species | $P$ ($m^{-3}$) | $P$ ($ml^{-1}$) | $\lambda$ ($\mu$m) | $L_p$ ($\mu$m) | Region, reference |
|---|---|---|---|---|---|
| Field observations | | | | | |
| *Nannochloris atomus* | $7.2 \times 10^{12}$ | $7.2 \times 10^{6}$ | 52 | 360 | Great South Bay (Hulburt 1970) |
| Total phytoplankton | $9.9 \times 10^{11}$ | $9.9 \times 10^{5}$ | 100 | 780 | Salt Pond, Woods Hole (Hulburt 1970) |
| *Cyclotella nana* | $5.5 \times 10^{11}$ | $5.5 \times 10^{5}$ | 122 | 850 | Great South Bay (Hulburt 1970) |
| Coccoid cyanobacteria | $3.4 \times 10^{11}$ | $3.4 \times 10^{5}$ | 143 | 1,000 | Gulf of Maine (Murphy and Haugen 1985) |
| *Selenastrum* sp. | $2.5 \times 10^{11}$ | $2.5 \times 10^{5}$ | 159 | 1,100 | Lake Elmenteita, East Africa (Melack 1988) |
| *Skeletonema costatum* | $6.0 \times 10^{8}$ | $6.0 \times 10^{3}$ | 1,186 | 8,300 | Off New York Harbor (Hulburt 1970) |
| Total phytoplankton | $2.3 \times 10^{8}$ | $2.3 \times 10^{3}$ | 1,632 | 11,300 | Station S, Bermuda (Hulburt *et al.* 1960) |
| Semicontinuous batch culture competition experiment (Fig. 1) | | | | | |
| Initial values | $10^{9}$ | $10^{3}$ | 1,000 | 7,000 | |
| *Synedra ulna* | $10^{10}$ | $10^{4}$ | 464 | 3,200 | |

counting error; e.g., Guillard 1973). If the cells are distributed in a cubic matrix, each separated by their mean separation scale ($\lambda$), 400 cells occupy a volume of about 7 ($=400^{1/3}$) mean free paths on a side. Thus, the parcel scale, $L_p$, is equal to

$$L_p = 7\lambda = 7P^{-1/3}, \quad (3)$$

where $P$ is the abundance of the plankton (in $m^{-3}$). The exact choice of the number of particles to be counted within a parcel volume has little bearing on the scaling analyses to follow.

The size of the parcel scale is inversely related to abundance. A parcel scale for an organism observed at an abundance of 1 $m^{-3}$ will be 7 m, whereas organisms with an abundance of 1 $ml^{-1}$ ($10^6$ $m^{-3}$) will be viewed as a continuous field if evaluated using a spatial scale larger than 7 cm. Values of $L_p$ will become quite large if the plankter is found only rarely; however, there will be a lower limit to $L_p$ values in nature given by the highest observed abundance. Extremely high phytoplankton abundance observations range from $5 \times 10^5$ to $10^6$ $ml^{-1}$, which corresponds to a minimum parcel scale of ~500 $\mu$m (Table 1). Thus, values of $L_p$ for natural populations of phytoplankton will be >500 $\mu$m. The maximum cell abundances given in Table 1 were culled from a variety of aquatic ecosystem investigations (although a recognized oceanographic bias remains).

By comparison, the largest $L_p$ values for nutrient molecules are <10 $\mu$m, which are considerably less than the smallest $L_p$ scales (>500 $\mu$m) found for natural phytoplankton distributions (Table 2). These maximum $L_p$ values are found in oligotrophic regions where recent analytical techniques have enabled the determination of nutrient concentrations as low as 1 nM (Table 2; e.g., Garside 1985; Brzezinski 1988). Thus, the largest parcel scale for nutrient molecules is typically 5 $\mu$m (Table 2), about 100 times smaller than 500-$\mu$m minimum $L_p$ value expected for phytoplankton distributions (Table 1).

## Planktonic organism populations as fluid variables

A fluid is a collection of molecules or particles whose mass, motion, and composition can be assessed by examining a small volume, a fluid element, rather than requiring a particle-by-particle (or molecule-by-molecule) analysis (e.g., Batchelor 1973; Tritton 1988). Thus, the dynamics of a fluid system can be completely diagnosed using macroscopic, or fluid, variables. Fluid variables are continuously distributed in space and time, and their spatial gradients of arbitrary order will also be continuous. Water is obviously a fluid. The billions and billions of molecules in a just 1 $\mu$l of water (actually, $\sim 3 \times 10^{19}$) illustrate that the effects of individual molecular trajectories, such as Brownian motions, are unimportant for evaluating the trajectory of this 1 $\mu$l of water as they are effectively averaged out over the many molecules considered. Hence, water itself satisfies the continuum hypothesis and is strictly a fluid.

Application of conservation of mass enables prognostic relationships for the concentration of any fluid constituent ($C_i(\vec{x}, t)$) to be developed, or

$$\frac{\partial C_i}{\partial t} + \vec{u} \cdot \nabla C_i = G_i(S_1, \ldots S_M, C_1, \ldots, C_N, \ldots), \quad (4)$$

Table 2. Smallest observed nutrient concentrations from a variety of aquatic environments. The minimal nutrient concentrations shown were from a survey of low-level nutrient determinations from a variety of aquatic ecosystems. Because it has the lowest possible nutrient conditions, which is the focus here, the observations shown are from the oligotrophic Sargasso Sea.

| Nutrient | $P$ ($m^{-3}$) | $P$ (nM) | $L_p$ ($\mu$m) | Region, reference |
|---|---|---|---|---|
| 1 $\mu$M anything | $6.0 \times 10^{20}$ | 1,000 | 0.8 | |
| Nitrate | $1.2 \times 10^{18}$ | 2 | 6.5 | Sargasso Sea (Garside 1985) |
| Ammonium | $1.8 \times 10^{18}$ | 3 | 5.7 | Sargasso Sea (Brzezinski 1988) |
| Nitrite | $4.2 \times 10^{17}$ | 0.7 | 9.3 | Sargasso Sea (Brzezinski 1988) |

Table 3. Typical flow length scales for various physical environments. Turbulent kinetic energy dissipation rates are based upon cruise averages of direct observations.

| Environments | $\epsilon$ ($m^2$ $s^{-3}$) | $10L_K$ ($\mu$m) | $10L_B$ ($\mu$m) | Reference |
|---|---|---|---|---|
| Ocean mixed layer | $10^{-4}$ | 3,200 | 120 | Oakley and Elliott 1982 |
| Lake mixed layer | $10^{-6}$ | 10,000 | 390 | Imberger and Ivey 1991 |
| Ocean seasonal thermocline | $10^{-6}$ | 10,000 | 390 | Gregg 1989 |
| Lake thermocline | $10^{-8}$ | 32,000 | 1,200 | Imberger and Ivey 1991 |
| Ocean main thermocline | $10^{-9}$ | 56,000 | 2,200 | Gregg 1989 |
| Continuously stirred 1-liter chemostat | 1 | 320 | 12 | |

where $\vec{u}(\vec{x}, t)$ is the three-dimensional velocity vector, $\nabla$ is the gradient operator ($=\mathbf{i}\partial/\partial x + \mathbf{j}\partial/\partial y + \mathbf{k}\partial/\partial z$), and $G_i(\ldots)$ represents the net production of $C_i(\vec{x}, t)$ as a function of limiting resource concentrations ($S_1, \ldots, S_M$) and resource concentrations found within each species ($C_1, \ldots, C_N$). This expression is identical to conservation relationships developed for heat or solute concentration (e.g., Tritton 1988) and states that local changes in the concentration of species $i(\partial C_i/\partial t)$ are due to advection by the flow field ($\vec{u}\cdot\nabla C_i$) and net production ($G_i(\ldots)$).

For a distribution of organisms to be considered a fluid variable and thereby satisfying the continuum hypothesis, the parcel scale must not be larger than any other relevant scale in the flow. Implications of this statement can be addressed by examining Eq. 4. First, continuous estimates of $\nabla C_i$ can be made only over spatial scales larger than $L_p$. Hence, advection can be quantified only over scales larger than $L_p$. Second, the flow field will act to advect individual organisms rather than move the entire population contained in $L_p$, if $\vec{u}(\vec{x}, t)$ varies on scales much smaller than $L_p$. Finally, if the limiting resource concentration, $S_k$, varies over scales smaller than $L_p$, neighboring organisms can experience differing substrate concentrations and hence different net production rates ($G_i(\ldots)$). Obviously, if these conditions are not met, the application of a conservation relationship such as Eq. 4 will not be valid.

The comparison of a species' parcel scale with the smallest relevant environmental length scale in the flow, $L_{\text{flow}}$, provides a simple criterion for whether the population may be considered a fluid variable. That is, if

$$L_p \ll L_{\text{flow}}, \tag{5}$$

then the organism's population density can be considered continuously distributed and fluid mechanical approaches for assessing changes in abundance, such as Eqs. 1 and 4, may be applied. If this criterion is not met, then the application of continuum methodology to this discrete collection of individual organisms must be carefully reexamined.

## Naturally occurring spatial scales in aquatic flows

Aquatic flows may be characterized by a myriad of length scales from basin-scale circulation patterns to microscopic scales, where molecular processes are dominant. Relevant to the present discussion, turbulent energy dissipation processes impose several important flow scales and hence are relevant to the present discussion of the interactions among planktonic particles (e.g., Tennekes and Lumley 1972; Denman and Gargett 1983; Gregg 1987; Imberger and Ivey 1991). For example, the Kolmogorov scale ($L_K$) may be used to characterize the size of the smallest turbulent eddies in a flow (e.g., Tennekes and Lumley 1972), which are thought to have a role in the feeding efficiency of zooplankton (cf., Rothschild and Osborn 1988; Granata and Dickey 1991). The Kolmogorov scale is defined as the scale where molecular viscous and turbulent inertial forces are the same magnitude in affecting the momentum of the flow field or

$$L_K = \left(\frac{\nu^3}{\epsilon}\right)^{1/4}, \tag{6}$$

where $\nu$ is the kinematic viscosity of water ($10^{-6}$ $m^2$ $s^{-1}$) and $\epsilon$ is the turbulent kinetic energy dissipation rate (in $m^2$ $s^{-3}$). Turbulence kinetic energy dissipation rates found in natural waters range from $10^{-4}$ to $10^{-9}$ $m^2$ $s^{-3}$ (Table 3), where large $\epsilon$ values typically occur near a boundary, the air–sea interface or benthos, and smaller values are found within the quiescent ocean interior (e.g., Gregg 1987, 1989). Observations suggest that the size of the smallest turbulent eddy will be about 10 times greater than $L_K$ (e.g., Gibson 1980; Oakey and Elliott 1982). Thus, turbulence will act to advect materials differentially for scales greater than $\sim 10L_K$. For a range of aquatic environments, typical values for $10L_K$ range from 3,200 to 56,000 $\mu$m (Table 3).

The smallest scale where turbulence creates fluctuations in the nutrient field corresponds to the Batchelor scale, $L_B$. The Batchelor scale is defined as the scale where the effects of Kolmogorov scale eddies on the nutrient field are balanced by the molecular diffusion of the nutrient (e.g., Batchelor 1959; Tennekes and Lumley 1972) or

$$L_B = \left(\frac{\kappa^2\nu}{\epsilon}\right)^{1/4}, \tag{7}$$

where $\kappa$ is the molecular diffusivity of the nutrient ($1.4 \times 10^{-9}$ $m^2$ $s^{-1}$ for $NO_3^-$ in seawater, which is similar to values for other dissolved ions). The derivation of Eq. 7 requires that the Schmidt number for the nutrient, defined as the ratio of molecular viscosity to diffusivity, is much greater than 1 (Batchelor, 1959). The Schmidt number for nitrate in seawater is $\sim$700. For present purposes, the Batchelor scale represents the smallest scales where spatial variations in a passive scalar will be found (assuming that it is a fluid variable). A reasonable upper bound for the scale of the smallest nutrient micropatch is about 10 times $L_B$ (e.g., Lazier and Mann 1989). Values of 10 $L_B$ for nitrate in seawater range from 120 to 2,200 $\mu$m for a wide range of environments

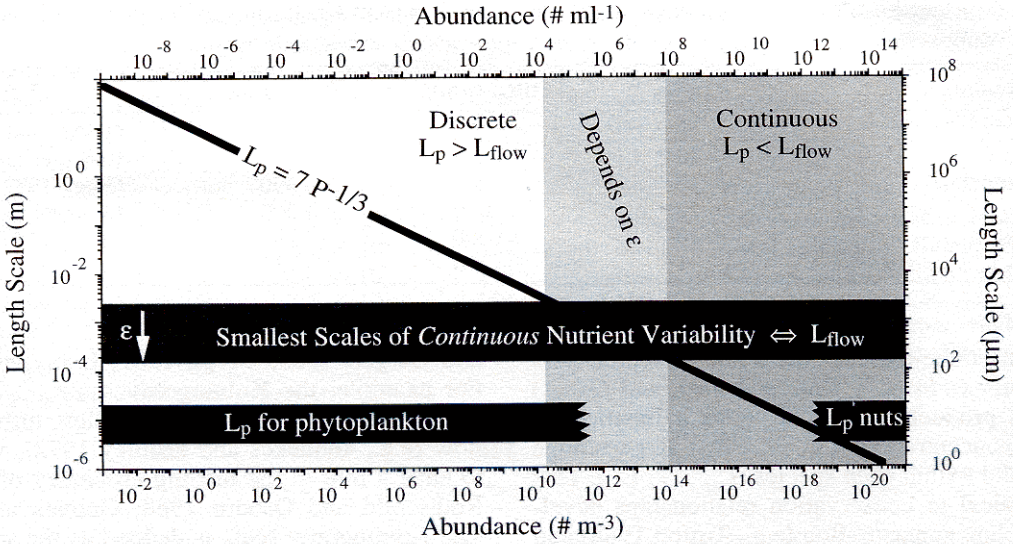


Fig. 3. Comparison between phytoplankton parcel scale ($L_p$) and ranges for the nutrient micropatch length scale ($L_{flow}$) for typical aquatic environments. If $L_p \ll L_{flow}$, the phytoplankton are distributed continuously; if $L_p \gg L_{flow}$, they are distributed discretely. Values of $L_{flow}$ decrease with increasing turbulent kinetic energy dissipation rates ($\epsilon$). The range of $L_{flow}$ values shown here is taken from Table 3.

(Table 3), and the larger nutrient micropatch scales correspond to environments with the lowest turbulent activity. The scale of the smallest nutrient micropatch (10 $L_B$) will be much smaller than the scale of the smallest turbulent eddy (10 $L_K$; Table 3). Hence, 10 $L_B$ will represent the smallest relevant flow scale, $L_{flow}$, for phytoplankton resource competition. For other ecological problems, other characteristic length scales may be more relevant (cf. $L_{flow} \sim 10\ L_K$ for zooplankton feeding).

In contrast to natural waters, turbulence levels in laboratory culturing apparatus are generally many orders of magnitude higher. A conservative estimate of the rate of kinetic energy dissipation in a continuously stirred, 1-liter culturing vessel can be made by assuming that 10 W of power are required to drive a magnetic stir bar and that only 10% of this electrical power is converted into fluid motion. The resulting kinetic energy dissipation rate estimate is 1 W $kg^{-1}$ (1 $m^2\ s^{-3}$). This rate of turbulent energy dissipation is roughly one million times larger than those found in natural waters (Table 3) and corresponds to a nutrient micropatch scale of approximately 12 $\mu$m. Only a few laboratory experiments have been performed to simulate environmentally relevant turbulence levels (Pasciak and Gavis 1975; Marrasé et al. 1990; Thomas and Gibson 1990).

## Can phytoplankton populations be considered fluid variables?

The answer to the above question can be found by examining the relationship between our estimates of $L_p$ and $L_{flow}$ as a function of numerical abundance (Fig. 3). The diagonal bold line in Fig. 3 is the relationship between $L_p$ and abundance (Eq. 3), and the horizontal shaded region represents the smallest scales characteristic of nutrient micropatches ($L_{flow}$; Table 3). If the parcel scale, $L_p$, is much less than $L_{flow}$, the fluid continuum criterion (Eq. 5) is satisfied and the population is distributed continuously. If not, the distribution is discrete. From an examination of Fig. 3, cells found at abundances greater than $7 \times 10^7$ $ml^{-1}$ will always be distributed continuously, whereas populations with abundances less than $2 \times 10^4$ $ml^{-1}$ are discrete. For a range of cell abundances ($2 \times 10^4$ to $7 \times 10^7$ $ml^{-1}$), the nature of the distribution is dependent upon the turbulent activity of the environment, where the smallest $L_{flow}$ values correspond to the highest turbulence levels.

Only for the greatest observed phytoplankton abundances (Table 1) will values of $L_p$ approach those for $L_{flow}$ (Fig. 3). Thus for nearly all environments and times, phytoplankton cells must be treated as discrete particles. This result is not surprising because there are many species of phytoplankton that are larger than the minimum nutrient micropatch scale. The lowest observed nutrient concentrations indicate that nutrient molecules are distributed continuously for all aquatic environments (Table 2). Therefore, phytoplankton cells are discrete particles utilizing a continuous nutrient field about them.

Discreteness in phytoplankton distributions has many implications. Most importantly, it means that formulations of phytoplankton growth and interaction based upon assuming that planktonic organisms are fluid variables (such as Eq. 4) are inappropriate for modeling phytoplankton population variations in natural waters. These models assume a priori that phytoplankton populations are distributed continuously where every cell will uniformly and instantaneously feel the effects of its neighbor. However, because estimates of $L_p$ (and $\lambda$) are almost always smaller than $L_{flow}$, adjacent phytoplankton cells will be found in different nutrient micropatches. These microscale spatial variations will greatly in-

fluence the manner in which organisms interact with the nutrient field and with each other.

Scales of nutrient micropatches will not be the relevant flow scales for evaluating all problems. For zooplankton feeding, the relevant $L_{flow}$ is the smallest scale over which turbulence randomly advects prey particles, or $\sim 10\ L_K$ (Eq. 6). Typical values of 10 $L_K$ range from 3,000 to 50,000 $\mu$m (Table 3). Hence, zooplankton or their prey will be continuously distributed if their concentration is $>10^4$ ml$^{-1}$, whereas they will be discretely distributed if their abundance is $<10$ ml$^{-1}$. The range of abundances between these limits (10–$10^4$ ml$^{-1}$) will be continuous or discrete depending upon the ambient turbulence intensity. Thus, zooplankton organisms themselves probably will be distributed discretely, whereas their prey (phytoplankton) are likely to be distributed continuously for this particular application. The resolution of this particular issue is beyond the scope of this contribution but is presented to illustrate the discrete nature of many aquatic ecosystems.

## Parameterizing discreteness

To understand properly phytoplankton competition in natural waters, the effects of discreteness must be taken into account. Although it is straightforward to simulate on a computer the dynamics of every phytoplankton cell in a numerical ecosystem, the computational task would be gargantuan. For example, a rather small lake (1 ha by 1 m deep, a volume of $10^4$ m$^3$) with an average organism abundance of 1 ml$^{-1}$ will contain $10^{10}$ distinct cells. A particle-following model for this small domain would daunt even the most capable supercomputer (e.g., Reynolds 1989). Clearly, the application of an individual-based simulation model for the Atlantic Ocean (a volume of $\sim 3.5 \times 10^{17}$ m$^3$) is unrealistic.

An alternative approach is to parameterize the effects of discrete interactions among individuals using population-level information. This approach would allow the community dynamics to be predicted while accounting for, maybe only in a statistical sense, the effects of discreteness. This problem is, in essence, a subgrid scale problem where the effects of unresolved discrete individual interactions on the larger, resolved spatial scales are parameterized in terms of community-level parameters. The present problem is analogous to the turbulence subgrid scale problem where the effects of small-scale mixing are parameterized in terms of eddy transport coefficients, which are often parameterized in terms of flow field variables (e.g., Gregg 1987; Lesieur 1987; Reynolds 1989; Siegel and Domaradzki 1994).

One approach to developing a community-level parameterization of discreteness would be to assess the spatial extent and time scale over which a single planktonic organism can influence the environment of its neighbors. Relevant to phytoplankton competition, the interplay between nutrient uptake and molecular diffusion creates a deficit in the nutrient field about a cell (e.g., Munk and Riley 1952). This local nutrient deficit can be used to define the extent of the sphere of influence that each phytoplankter instantaneously has on its immediate environment. If adjacent particles have overlapping spheres of influence, then the phytoplankton cells will be competing directly and instantaneously with one another for a local pool of nutrients (Fig. 4), whereas if their spheres of influence do not overlap, they will not compete directly. This idea of discrete phytoplankton competition was first suggested by Hulburt (1970).

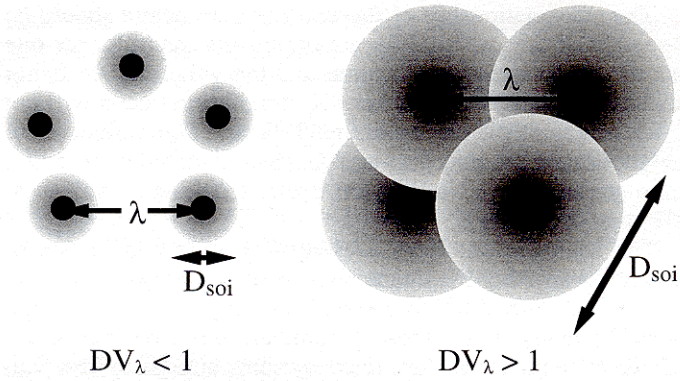


Fig. 4. The interaction of "spheres of influence" for a community of planktonic organisms. The situation on the right shows an example where the cell's sphere of influence ($D_{soi}$) is of the same order as the mean free path separating particles ($\lambda$). For this case, spheres of influence overlap and adjacent organisms can compete for resources. On the left is the situation where $D_{soi}$ is less than $\lambda$. Here, adjacent spheres of influence do not overlap and competition is not predicted.

This concept of overlapping spheres of influence can be evaluated using a single parameter, the spatial distribution variable ($DV_\lambda$). $DV_\lambda$ is defined as the ratio of the diameter of a particle's sphere of influence ($D_{soi}$) to the mean free path between adjacent particles ($\lambda$), or

$$DV_\lambda \equiv \frac{D_{soi}}{\lambda}. \tag{8a}$$

If $DV_\lambda$ is $>1$, adjacent spheres of influence are overlapping for all time periods and neighboring planktonic organisms will compete with one another, whereas if estimates of $DV_\lambda$ are $<1$, adjacent cells will be too far apart to compete effectively and they will not feel the effects of their neighbors. However, when evaluated over longer time scales (such as a division cycle), an organism may still be influenced by its neighbors. To quantify the relative importance of time scales, a temporal distribution variable ($DV_\tau$) is defined as the ratio of a characteristic biological time scale for the organism ($\tau_{bio}$) to the time scale that an organism will feel the effects of its neighbors, ($\tau_\lambda$), or

$$DV_\tau \equiv \frac{\tau_{bio}}{\tau_\lambda}. \tag{8b}$$

If the value of $DV_\tau$ is $\geq 1$, the organism's biological time scale is longer than the temporal scale that characterizes the influence of its neighboring cells. Hence, adjacent organisms will be able to feel the effects of each other over the organisms' intrinsic time scale. However, if $DV_\tau$ is much less than 1, then neighboring organisms will be independent of one another over a single generation. Alternatively, values of $DV_\tau$ may be defined using the ratio of relevant physical and biological nutrient transport rates.

The interrelationship of the two $DV$ parameters should be apparent. If $DV_\lambda$ is $>1$, adjacent organisms can influence one another at every instant of time and the value of $DV_\tau$ is not relevant. If values of $DV_\lambda$ are $<1$, neighboring cells will not affect each other on a continual basis. The influence of neighboring cells may still be felt when assessed over longer time scales, such as a division cycle, resulting in values of $DV_\tau$ that are order 1.

The scaling arguments presented here provide a set of useful parameters for characterizing phytoplankton competition on the time and space scales of the individual organisms. In many ways, these parameters describe the effects of discreteness in planktonic ecosystems similar to how values of Reynolds numbers describe the turbulent vs. laminar nature of a flow field. As presented, the definitions of the spatial and temporal distribution variables are general and may be easily extended to other ecological and demographic systems.

## Parameterizing distribution variables for phytoplankton competition

Application of the $DV$ parameters to a natural ecosystem requires order of magnitude estimates for $D_{soi}$, $\tau_{bio}$, and $\tau_\lambda$. At the scales of individual organisms, the physical transport of dissolved nutrients will be regulated by low Reynolds/Peclet number dynamics where molecular diffusion processes are dominant (e.g., Vogel 1981). This is fortunate because diffusion processes are often straightforward to diagnose theoretically.

To estimate the spatial distribution variable ($DV_\lambda$) parameter, the diameter of a organism's sphere of influence ($D_{soi}$) and its mean separation from neighboring cells ($\lambda$) must be determined. The organism's abundance provides an estimate of $\lambda$ ($P^{-1/3}$); however, it is difficult to unambiguously define $D_{soi}$. For the case of phytoplankton competition, values for $D_{soi}$ can be estimated by determining the extent of the diffusion-driven boundary layer about a cell. This boundary layer is created by a balance between the diffusive transport of nutrients to the cell wall and the cell's intrinsic nutrient uptake rate. In general, this length scale is a function of the size and shape of the plankter, its uptake kinetics, motility, and sinking characteristics, the ambient turbulence intensity, and the molecular diffusivity of the nutrient (e.g., Munk and Riley 1952; Pasciak and Gavis 1974, 1975; Berg and Purcell 1977; Sommer 1988; Lazier and Mann 1989). For the simplest case, a spherical, motionless cell is absorbing nutrients at a rate specified by the cell's nutrient transport system and the nutrient concentration at the cell wall. At steady state, the cell's nutrient uptake rate is balanced by the transport of nutrient to the cell wall by molecular diffusion. The radial distribution of nutrient substrate, $S(r)$, may be determined by assuming that the radial divergence of the diffusive nutrient transport is zero $[\partial(r^2\partial S/\partial r)/\partial r = 0]$ or by solving for $S(r)$,

$$S(r) = S_\infty + \left(\frac{R}{r}\right)[S(R) - S_\infty] = S_\infty - \left(\frac{R}{r}\right)\Delta S, \quad (9)$$

where $r$ is the radial distance from the center of the cell, $R$ is the radius of the cell, $S(R)$ is the nutrient concentration at the cell wall, $S_\infty$ is the ambient or far-field nutrient concentration, and $\Delta S$ is the nutrient deficit at the cell wall because of cellular uptake $[\Delta S = S_\infty - S(R)]$. This expression is valid only for $r \geq R$ (Fig. 5). A convenient measure for $D_{soi}$ is twice the radial distance ($r_{90}$), where the concentration of nutrient is 90% of the far-field concentraiton $[S(r_{90}) = 0.90S_\infty]$. This length scale definition is analogous to the definition of a boundary layer thickness (e.g., Batchelor 1973) and is equal to

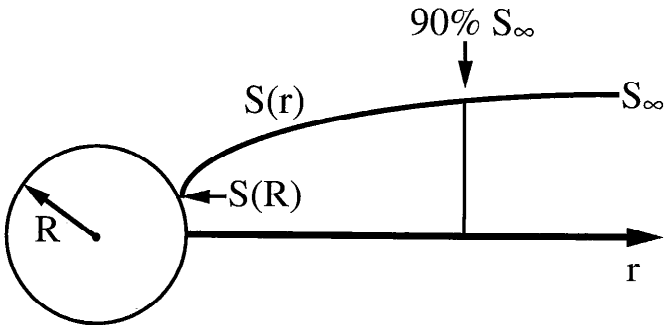


Fig. 5. The sphere of influence around a single phytoplankter. The diameter of the sphere of influence ($D_{soi}$) is defined here as twice the radial distance ($r_{90}$) where the local nutrient concentration is 90% of the ambient or far-field nutrient concentration ($S_\infty$).

$$r_{90} = 10R\left(\frac{\Delta S}{S_\infty}\right) \quad (10a)$$

under the provision that $r_{90}$ is greater than the radius of the cell (Fig. 5). Using this definition, the diameter of a cell's sphere of influence, $D_{soi}$, may be determined using the diameter of the spherical cell, $D_{cell}$, or

$$D_{soi} = 10D_{cell}\left(\frac{\Delta S}{S_\infty}\right) = 10D_{cell}\left[\frac{S_\infty - S(R)}{S_\infty}\right], \quad (10b)$$

where $D_{soi} \geq D_{cell}$. Thus, $D_{soi}$ is directly proportional to the normalized nutrient deficit created at the cell wall and the diameter of the cell. If $S(R)$ is equal to zero, $D_{soi}$ will be at its maximal extent ($10D_{cell}$), whereas the smallest possible $D_{soi}$ equals $D_{cell}$. Here, I assume that $D_{soi}$ is equal to $5D_{cell}$. The error caused by this assumption will be small because of the limited range of possible values for $D_{soi}$ ($D_{cell} \leq D_{soi} \leq 10D_{cell}$).

The diffusion-based theory presented applies only in the case of motionless spherical cell in a quiescent fluid. Relative motions of the cell will thin the diffusive boundary layer, increasing the rate of supply of nutrients to the cell wall. These relative motions may be driven by cellular motility, Stokes sinking, turbulence-generated shears on the scale of the cell, or simply fluid mechanical slippage of a cell through its water parcel (e.g., Munk and Riley 1952; Pasciak and Gavis 1974; Berg and Purcell 1977; Sommer 1988; Lazier and Mann 1989; Granata and Dickey 1991; Siegel and Plueddemann 1991). The net effect of these relative motions will be to reduce the extent of the diffusive boundary layer, thereby reducing $D_{soi}$. Because $D_{soi}$ cannot be less than $D_{cell}$,

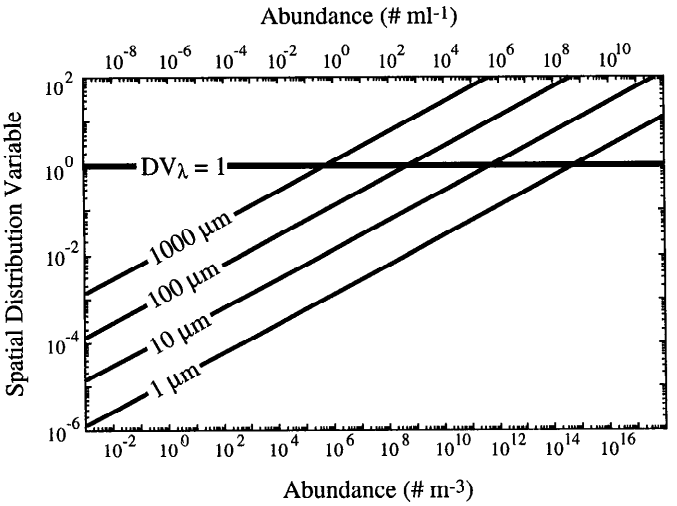


Fig. 6. Relationship between the spatial distribution variable ($DV_\lambda$) and cellular abundance for cell diameters ranging from 1 to 1,000 $\mu$m (Eq. 11). The different cell diameters are shown by the diagonal lines. If $DV_\lambda > 1$, direct competition for resources among neighboring cells can occur. However, if $DV_\lambda < 1$, direct competition is not expected.

the estimate of $5D_{cell}$ for $D_{soi}$ is probably a slight overestimate.

Using the above estimate of $D_{soi}$, values of the spatial distribution variable ($DV_\lambda$) for phytoplankton competition in natural waters can be determined as

$$DV_\lambda = 5D_{cell}P^{1/3}, \quad (11)$$

where $P$ is the phytoplankton abundance (in $m^{-3}$). A graphical representation of Eq. 11 is given in Fig. 6 for cell diameters ranging from 1 to 1,000 $\mu$m. Large values of $DV_\lambda$ occur when large cells are found at great abundances, which occurs rarely for naturally phytoplankton populations (Fig. 6, Table 1). For example, picoplankton cells ($D_{cell} \sim 1$ $\mu$m) will compete only if their abundance is $>10^9$ $ml^{-1}$ (Fig. 6), which is several orders of magnitude greater than any of the highest observed abundances (Table 1). Thus, picoplankton cells will infrequently compete with one another for local nutrient supplies (although the question of how infrequently remains). However, values of $DV_\lambda$ for 100-$\mu$m-diameter cells approach 1 at an abundance of 1,000 $ml^{-1}$. Net phytoplankton have been observed at these abundances (Table 1), suggesting that competition can be direct and instantaneous.

Phytoplankton abundances used in most laboratory competition experiments often result in unrealistically high $DV_\lambda$ values. For example, the $DV_\lambda$ value for the final state of the competition experiment shown in Fig. 1 is approximately 1 (based upon $D_{cell} = 100$ $\mu$m and $P = 10^4$ $ml^{-1}$). Laboratory simulations are often high $DV_\lambda$ environments and will not correctly represent natural conditions.

Determination of the temporal distribution variable ($DV_\tau$) requires knowledge of two relevant time scales; a characteristic biological time scale for the organism ($\tau_{bio}$) and the time required for a neighboring organism to feel the effects of its neighbors ($\tau_\lambda$). For the case of nutrient competition, estimates of $DV_\tau$ can be better stated as the ratio of relevant rates; the rate at which neighboring cells are intercepting a given cell's potential nutrient supply in relation to the cell's intrinsic nutrient demand over its division cycle, or

$$DV_\tau = \frac{\text{intercepted nutrient supply}}{\text{cellular nutrient demand}}. \quad (12)$$

If $DV_\tau$ is much less than 1, adjacent cells will not influence the nutrient supply expected by a cell during its division cycle. However, if $DV_\tau$ approaches 1, neighboring cells will have reduced significantly the nutrient requirement of a phytoplankter.

A cell's nutrient demand can be estimated knowing the amount of nutrient required to undergo a division and the cell's characteristic division time ($\tau_{div}$). Alternatively, at steady state a cell's nutrient demand must balance the diffusive transport of nutrients towards the cell. The diffusive nutrient transport rate at the cell wall (in mole $N$ per unit time) is equal to $\pi D_{cell}^2 (-\kappa \partial S/\partial r|_{r=D_{cell}})$, which can be expressed as $2\pi\kappa D_{cell}\Delta S$ using Eq. 9. An estimate of the cellular nutrient demand intercepted by $N_n$ neighboring cells can also be estimated using diffusion theory. The diffusive flux at a distance $\lambda$ from a given cell is defined as $-\kappa \partial S/\partial r|_{r=\lambda}$, which can be expressed as $\kappa \Delta S D_{cell}/(2\lambda^2)$ (in mole $N$ per area per unit time). Each neighboring cell will intercept this flux with a cross-sectional area of $\pi D_{soi}^2/4$ (or $25/4\pi D_{cell}^2$ using the approximation, $D_{soi} = 5D_{cell}$). Thus, the estimate for the nutrient demand intercepted by $N_n$ neighboring cells is $(25/8)N_n\pi\kappa\Delta S D_{cell}^3/\lambda^2$. The resulting estimates for $DV_\tau$ are

$$DV_\tau = \frac{(25\pi/8)N_n\kappa\Delta S D_{cell}^3/\lambda^2}{2\pi\kappa D_{cell}\Delta S} = \frac{25}{16}N_n D_{cell}^2 P^{2/3}, \quad (13)$$

where the relationship between abundance ($P$) and mean free path is used ($\lambda \equiv P^{-1/3}$). In the following, I assume that there are six neighbors ($N_n$) surrounding the cell consistent with our method for estimating $\lambda$.

For the case of phytoplankton competition for a limiting nutrient substrate, estimates of the value of $DV_\tau$ can be parameterized as functions of the phytoplankton abundance, $P$, and the diameter of a cell, $D_{cell}$ (Fig. 7). Again, large values of $DV_\tau$ occur when large cells are found at great abundances. For relatively large phytoplankton cell sizes, which often characterize eutrophic environments ($D_{cell} \sim 100$ $\mu$m), values of $DV_\tau$ become appreciable (0.01) for abundances greater than $\sim 30$ $ml^{-1}$ and are order 1 when $P$ is $\sim 30{,}000$ $ml^{-1}$. Net phytoplankton are often observed at abundances $>1{,}000$ $ml^{-1}$ and rarely with abundances $>10{,}000$ $ml^{-1}$ (Table 1), which suggests that competition for a limiting nutrient substrate can occur for large phytoplankton species ($D_{cell} \geq 100$ $\mu$m) at fairly high abundances ($P \geq 1{,}000$ $ml^{-1}$). However, picoplankton cells ($D_{cell} = 1$ $\mu$m) will only begin to compete if their cellular abundances are greater than $\sim 5 \times 10^7$ $ml^{-1}$ (Fig. 7). Picoplankton abundances this large are not found in nature (Table 1), and picoplankton-size cells will only be marginally influenced by their neighbors throughout their division cycle.

The two $DV$ scaling parameters together demonstrate that rates of resource competition will be, to first order, a function of the phytoplankton abundance and size of the phytoplankton cells in question. Ecosystems characterized by larger

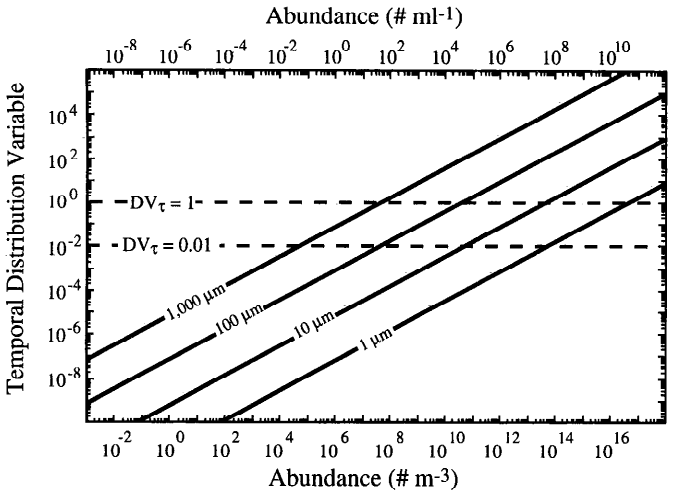


Fig. 7. Relationship between the temporal distribution variable ($DV_\tau$) for phytoplankton-nutrient competition and phytoplankton abundance for cell diameters ranging from 1 to 1,000 $\mu$m (Eq. 13). It is assumed that there are six neighbors ($N_n$) surrounding the cell. If $DV_\tau$ approaches 1, neighboring cells can affect each other's nutrient supply over a division time. However, if $DV_\tau \ll 1$, competition is not expected.

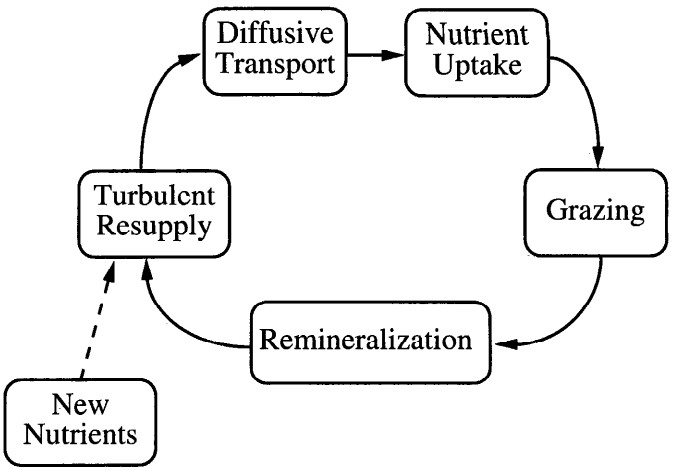


Fig. 8. The linked cycle of nutrient flux processes that are required for the present idealization of a steady state oligotrophic ecosystem. No new sources of nutrients are considered. At steady state, the nutrient flux through each process must be balanced. However, if the ecosystem is not at steady state, the flux processes shown here are not required to be in balance and materials can accumulate within the various pools of the cycle.

phytoplankton species ($D_{cell} \geq 100$ $\mu$m) are likely sites for nutrient competition when abundances are greater than ~100 ml$^{-1}$. However, for oligotrophic ecosystems dominated by small phytoplankton cells, rates of competition will be greatly reduced from those predicted by resource competition theory (Eq. 1a–c).

## Scenarios for discrete resource competition

The microscale phytoplankton competition model introduced here makes some important predictions for the role of phytoplankton competition in natural waters and provides a simple resolution for Hutchinson's (1961) paradox of the plankton. To simplify the following discussion, I define, without proof, a community-based $DV$ parameter. $\Sigma DV$, which will account for the combined effects of $DV_\lambda$ and $DV_\tau$ for a community of phytoplankton. The exact method for making this transformation is an open question, although values of $\Sigma DV$ will be an increasing function of cell abundance and size. The basic interpretation of the scaling analysis will remain the same as the community-level $DV$ parameter, $\Sigma DV$, is applied to assess microscale interactions for several important planktonic ecosystems.

First, the microscale interactions within an idealization of a steady state planktonic oligotrophic ecosystem are examined. For this environment, ambient nutrient concentrations and phytoplankton abundances are low and the dominant phytoplankters are generally nanoplankton and smaller ($D_{cell} \leq 10$ $\mu$m; e.g., Murphy and Haugen 1985; Chisholm 1992). The resulting $\Sigma DV$ values should be much less than 1 and individual phytoplankton cells will grow by independently utilizing their local nutrient concentrations. Because this is a steady state ecosystem, the community averaged nutrient uptake rate must equal the rate that grazing and remineralization processes recycle these nutrients. Thus, there exists a linked cycle of processes that describes nutrient flow through this community (Fig. 8). This cycle is closed by a mechanism (i.e., turbulence) that transports nutrients from the sites of the individual grazing–remineralization events to the individual phytoplankton cells.

The time and space scales for grazing–remineralization events have an important role in maintaining phytoplankton diversity in an oligotrophic eocsystem. If grazing events are sporadic and separated by huge intercellular distances, grazing, remineralization, and intercellular nutrient transport processes act to randomize the supply of nutrients to the individual phytoplankton cells. However, if these events occur uniformly in space and time, the growth of each cell will be identical because they will respond to the same nutrient supply rate. A hint of these space/time scales may be derived by examining their parameterization in the competition equations (Eq. 1a–c), or

$$\left(\frac{dC}{dt}\right)_{loss} = -mC, \tag{14}$$

where $C$ is the nutrient content in phytoplankton and $m$ is the grazing–remineralization rate. For small changes in time ($\Delta t \ll m^{-1}$), the fractional change in $C(\Delta C/C)$ is equal to $m\Delta t$ (which is equivalent to the fractional change in abundance assuming a constant cell quota). For a phytoplankton grazing rate of $1d^{-1}$, 1 cell out of 86,400 will be grazed and remineralized each second. The length scale separating these events will be >40 times [86,400)$^{1/3}$] larger than the algal cell separation scale, $\lambda$, which corresponds to a spatial scale of 44 cm for an abundance of 1 ml$^{-1}$. Thus, grazing–remineralization events will be intermittent in time and space, which randomizes the resupply of recycled nutrients to in-

dividual phytoplankton cells. Because turbulence cannot discriminate among the various algal species present, it is unlikely that competitive exclusion due to nutrient competition can occur in an oligotrophic ecosystem. For exclusion displacements to occur, one species must be grazed consistently and receive no recycled nutrient to support its growth. It seems much more likely that the stochastic nature of the grazing–remineralization events, as well as the turbulent resupply processes, will preclude this possibility. Further, the low $\Sigma DV$ values characterizing the oligotrophic environment indicate that rates of cellular nutrient demand will be unaffected by neighboring cells. Hence, both mechanisms predict a tendency towards neutral stability for an oligotrophic phytoplankton assemblage.

The present idealization of an oligotrophic ecosystem assumes steady state conditions. This means that the flux through each process of the nutrient cycle illustrated in Fig. 8 is in exact balance. If the system is not in steady state, one of the linkages between the coupled processes is broken and materials can accumulate within the possible pools. The input of new nutrients into an initially low $\Sigma DV$ assemblage is an important example of an unsteady aquatic ecosystem. Rapid inputs of new nutrients can occur by a variety of processes, including vertical entrainment, wind-driven upwelling, convective mixing, lateral transport, and rain deposition (e.g., Sverdrup 1953; Klein and Coste 1984; Siegel et al. 1990; Michaels et al. 1993). For this unsteady ecosystem, nutrients are taken up by the cells and their abundance increases. The increased ambient nutrient conditions also enable the larger phytoplankton cells in an assemblage to grow more rapidly (e.g., Banse 1976; Sommer 1983). The resulting estimates of $\Sigma DV$ will increase correspondingly, leading to competition among individual phytoplankton cells for the limiting nutrients. In time, this competition can lead to a reduction in the community's diversity because of competitive displacement. This transition to competitive dynamics will occur for robust and mature algal blooms, where the new nutrient supply can support the escalating needs of the community. Laboratory competition experiments may be characterized by high $\Sigma DV$ values and result in species abundance dynamics that are accurately predictable using resource competition theory.

If the rate of new nutrient supply cannot keep pace with the demands of the phytoplankton community, the ambient nutrient concentrations must decrease in time, as would be expected because values of $\Sigma DV$ are initially of order 1. The coupled cycle of nutrient redistribution processes (Fig. 8) is broken because nutrient recycling and resupply rates cannot keep pace with the increasing nutrient demands of the community and the pool of dissolved inorganic nutrients must decrease in time. As ambient nutrient levels drop, the community will slowly shift to the discrete oligotrophic case and values of $\Sigma DV$ will decrease.

The microscale competition model here makes a serious prediction concerning Hutchinson's (1961) paradox of the plankton. The present scaling analysis and the previous arguments concerning the stochastic nature of the nutrient resupply process indicate that rates of resource competition will be greatly reduced for low $\Sigma DV$ conditions. Hence, little change in diversity in a steady state oligotrophic community should be expected. This is not saying that coexistence is expected for a low $\Sigma DV$ environment because only neutral stability of the assemblage is predicted (and then for $\Sigma DV \rightarrow 0$). Hence, the final outcome of competition may not be changed, only the time required to achieve that outcome. For these conditions, exclusion is likely to take so long that other processes will be more important than resource competition in determining the diversity of the community. These processes may include temporal fluctuations in the new nutrient supply, imposed diel cycles, and specialization of the grazer community. Thus, the microscale competition model provides a simple explanation of Hutchinson's (1961) paradox of the plankton by providing quantifiable bounds for the application of resource competition and its result, competitive exclusion, to natural planktonic ecosystems.

## Modeling planktonic ecosystems

The inapplicability of mass conservation approaches, such as resource theory, to the modeling of low $\Sigma DV$ phytoplankton assemblages raises the question of how should these systems be modeled. Plankton-following models will not be of much direct application because of their intensive computational demands. Hence, we need to evaluate the effects of discreteness on the temporal evolution of a community by developing discreteness indices, which may be evaluated using community-level information. We must solve the ecological subgrid scale (SGS) problem.

A first order SGS model for phytoplankton competition can be constructed by recognizing the effects of discreteness on rates of phytoplankton competition. If $\Sigma DV$ is large, the effects of discreteness are not important, and resource-based competitition expressions (Eq. 1a–c) may be applied without alteration. However if $\Sigma DV$ values are much less than 1, there should be minimal rates of resource competition. To account for discreteness, the resource-based competition theory (Eq. 1a–c) can be recast with an additional ad hoc factor, $\mathrm{SGS}_{DVi}$, which accounts for the effects of discreteness. An example for changes in the concentration of nutrient in the $i$th component of an phytoplankton assemblage would look like

$$\frac{dC_i}{dt} = \mathrm{SGS}_{DVi}\left(\frac{V_{mi}S}{K_i + S}C_i - mC_i\right), \tag{15}$$

where the parameters $C_i$, $K_i$, $V_{mi}$, and $m$ are defined as before (see Eq. 1a–c).

A reasonable first guess for the functional relationship of $\mathrm{SGS}_{DVi}$ on $\Sigma DV$ is shown in Fig. 9. The limiting behavior of $\mathrm{SGS}_{DVi}$ should be apparent. If the value of $\Sigma DV$ is $<1$, $\mathrm{SGS}_{DVi}$ should be $<1$ and temporal changes in $C_i$ will be less than predicted using vital rate information alone. Whereas if $\Sigma DV \geq 1$, then $\mathrm{SGS}_{DVi} = 1$.

Obviously, the details of the $\mathrm{SGS}_{DVi}$ relationship are unknown at this time. Even its functional form is questionable. To answer these questions, much new experimentation is required. For example, empirical determinations of $\mathrm{SGS}_{DVi}$ can be made by performing laboratory experiments at environmentally relevant turbulence intensities and cell abundances. Progress may also be made by performing detailed numer-

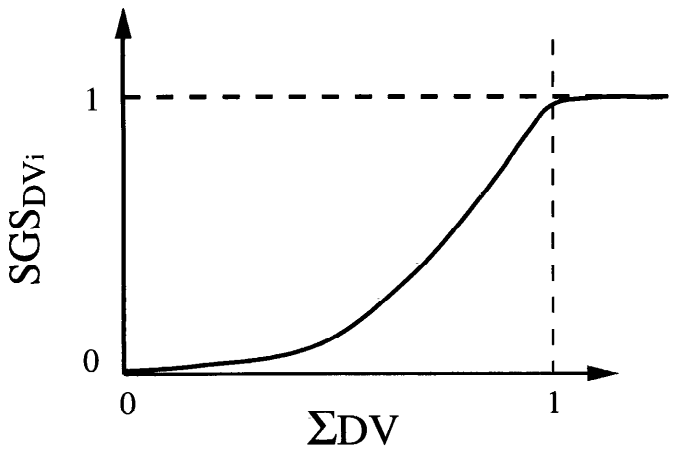


Fig. 9. A first order SGS model for describing the effects of discreteness in resourse-based competition models. $SGS_{DVi}$. The important parameter is the community level *DV* parameter, $\Sigma DV$. Values of $SGS_{DVi}$ will be large only if the $\Sigma DV$ is of order 1. Whereas for small $\Sigma DV$, values of $SGS_{DVi}$ will be small. Again, the functional relationship shown is only an educated guess.

ical experiments using individual particle-following models (e.g., Yamazaki et al. 1991; Blackburn et al. 1997). Although these models will not be useful for simulating any ecosystem of reasonably size, their application for examining ecosystem dynamics for small domains may be important for determining functional relationships for $SGS_{DVi}$. For the particular problem of zooplankton feeding, excellent examples of this approach have been proposed (e.g., Rothschild 1991; Davis et al. 1991).

In a sense, the present solution to the discreteness problem is similar to SGS parameterizations used for evaluating the effects of turbulence in fluid flows. In the simulation of a turbulent flow, spatial covariation within the unresolved or SGS velocity field gives rise to SGS Reynolds stresses (e.g., Leonard 1974; Lesieur 1987; Siegel and Domaradzki 1994). These SGS Reynolds stresses must be parameterized in terms of resolved scale flow field if the equations of fluid motion are to be solved. Here the unresolved covariation among the location of phytoplankton cells and the microscale nutrient fields gives rise to the ecological SGS problem.

## A final comment

The numerical modeling of plankton population changes may be problematic unless the ecological SGS problem is solved. Plankton biologists have long used detailed numerical models to investigate phytoplankton and zooplankton population variability (e.g., [illegible]ley et al. 1949; Steele 1974; Fasham et al. 1990). However, because these models have been formulated assuming that each pool (i.e., phytoplankton, zooplankton, etc.) is distributed continuously, these models will predict rates of material transfer between pools that are too fast if values of $\Sigma DV$ are $<1$. Hence, models of this type probably will not be able to correctly model plankton species distributions for all conditions.

As we all know (and would probably rather not admit), there is a certain amount of "art" involved in developing a numerical model for any ecosystem. There are many poorly understood physical and biological processes that must be represented mathematically (cf. mixing, grazing, remineralization, dissolved organic pool dynamics, etc.). These processes are often parameterized using adjustable constants that are determined by examining how a given model "works" compared with observations. In this way, many of these interaction terms are simply "fit" to match observations. However, the results of this curve fitting exercise solve not only their intended problem (parameterization of grazing rates, uptake, etc.) but the ecological SGS problem as well. Thus, although the SGS problem is not accounted for explicitly, it is accounted for implicitly if the interaction terms in the given model are determined empirically. Unfortunately, this does not mean that these models will work if applied to another site or time.

Detailed ecosystem models are beginning to be used to evaluate the roles of aquatic environments in the global biogeochemical cycling of materials with important global policy implications (e.g., IPCC 1995; Sarmiento and Lequere 1996). If these models are to accurately accomplish their intended tasks, they must hold for naturally occurring values of all relevant ecosystem parameters, which includes the $\Sigma DV$ parameter. The ecological SGS problem must be solved. Only by developing mechanistic ecosystem models that explicitly account for naturally occurring microscale interactions among individual organisms will plankton populations be predicted from a causal rather than a correlative basis.

## *References*

BANSE, K. 1976. Rates of growth, respiration and photosynthesis of unicellular algae as related to cell size. J. Phycol. **12:** 135–140.

BATCHELOR, G. K. 1959. Small-scale variation of convected quantities like temperature in turbulent fluid. J. Fluid Mech. **5:** 113–133.

———. 1973. An introduction to fluid dynamics. Cambridge Univ. Press.

BERG, H. C., AND E. M. PURCELL. 1977. The physics of chemoreception. Biophys. J. **20:** 193–219.

BLACKBURN, N., F. AZAM, AND A. HAGSTROM. 1997. Spatially explicit simulations of a microbial food web. Limnol. Oceanogr. **42:** 613–622.

BRZEZINSKI, M. A. 1988. Vertical distribution of ammonium in stratified oligotrophic waters. Limnol. Oceanogr. **33**: 1176–1182.

———, AND D. M. NELSON. 1988. Interactions between pulsed nutrient supplies and a photocycle affect phytoplankton competition for limiting nutrients in long-term culture. J. Phycol. **24:** 346–356.

CHISHOLM, S. W. 1992. Phytoplankton size, p. 213–237. *In* P. Falkowski [ed.], Primary productivity and biogeochemical cycles in the sea. Plenum.

DAVIS, C. S., G. R. FLIERL, P. H. WIEBE, AND P. J. S. FRANKS. 1991. Micropatches, turbulence and recruitment in plankton. J. Mar. Res. **49:** 109–151.

DENMAN, K. L., AND A. E. GARGETT. 1983. Time and space scales of vertical mixing and advection of phytoplankton in the upper ocean. Limnol. Oceanogr. **28:** 801–815.

FASHAM, M. J. R., H. W. DUCKLOW, AND S. M. MCKELVIE. 1990.

A nitrogen-based model of plankton dynamics in the oceanic mixed layer. J. Mar. Res. **48:** 591–639.

GARSIDE, C. 1985. The vertical distribution of nitrate in the open ocean surface water. Deep-Sea Res. **32:** 723–732.

GIBSON, C. H. 1980. Fossil temperature, salinity and vorticity turbulence in the ocean, p. 221–257. *In* J. C. J. Nihoul [ed.], Marine turbulence. Elsevier.

GRANATA, T. C., AND T. D. DICKEY. 1991. The fluid mechanics of copepod feeding in a turbulent flow: A theoretical approach. Prog. Oceanogr. **26:** 243–261.

GREGG, M. C. 1987. Diapycnal mixing in the thermocline: A review. J. Geophys. Res. **92:** 5249–5286.

———. 1989. Scaling turbulent dissipation in the thermocline. J. Geophys. Res. **94:** 9686–9698.

GUILLARD, R. R. L. 1973. Division rates, p. 289–311. *In* J. R. Stein [ed.], Handbook of phycological methods. Cambridge Univ. Press.

HULBURT, E. M. 1970. Competitiion for nutrients by marine phytoplankton in oceanic, coastal and estuarine regions. Ecology **51:** 475–484.

———, J. H. RYTHER, AND R. R. L. GUILLARD. 1960. The phytoplankton of the Sargasso Sea off Bermuda. J. Cons. Cons. Perm. Int. Explor. Mer. **25:** 115–128.

HUTCHINSON, G. E. 1961. The paradox of the plankton. Am. Nat. **95:** 137–145.

IMBERGER, J., AND G. N. IVEY. 1991. On the nature of turbulence in a stratified fluid 2, Application to lakes. J. Phys. Oceanogr. **21:** 659–680.

IPCC. 1995. Climate change 1995, the science of climate change, p. 572. J. T. Houghton and others [eds.], Contribution of Working Group I to the second assessment report of the Intergovernmental Panel on Climate Change. Cambridge Univ. Press.

KEMP, W. M., AND W. J. MITSCH. 1979. Turbulence and phytoplankton diversity: A general model of the "paradox of the plankton." Ecol. Modell. **7:** 201–222.

KLEIN, P., AND B. COSTE. 1984. Effects of wind-stress variability on nutrient transport into the mixed layer. Deep-Sea Res. **31:** 21–37.

LAZIER, J. R. N., AND K. H. MANN. 1989. Turbulence and the diffusive layers around small organisms. Deep-Sea Res. **36:** 1721–1733.

LEONARD, A. 1974. Energy cascades in large eddy simulations of turbulent fluid flows. Adv. Geophys. **18:** 237–248.

LESIEUR, M. 1987. Turbulence in fluids, p. 286. Nijhoff.

MARRASÉ, C., J. H. COSTELLO, T. GRANATA, AND J. R. STRICKLER. 1990. Grazing in a turbulent environment: Energy dissipation, encounter rates, and efficacy of feeding currents in *Centropages hamatus*. Proc. Natl. Acad. Sci. USA **87:** 1653–1657.

MELACK, J. M. 1988. Primary producer dynamics associated with evaporative concentration in a shallow, equatorial soda lake (Lake Elmenteita, Kenya). Hydrobiologia **158:** 1–14.

MICHAELS, A. F., D. A. SIEGEL, R. JOHNSON, A. H. KNAP, AND J. N. GALLOWAY. 1993. Episodic inputs of atmospheric nitrogen to the Sargasso Sea: Contributions to new production and phytoplankton blooms. Global Biogeochem. Cycles **7:** 339–351.

MURPHY, L. S., AND E. M. HAUGEN. 1985. The distribution and abundance of phototrophic ultraplankton in the North Atlantic. Limnol. Oceanogr. **30:** 47–58.

MUNK, W. H., AND G. A. RILEY. 1952. Absorption of nutrients by aquatic plants. J. Mar. Res. **11:** 215–240.

OAKEY, N. S., AND J. A. ELLIOTT. 1982. Dissipation within the surface mixed layer. J. Phys. Oceanogr. **12:** 171–185.

———, AND ———. 1975. Transport limitation nutrient uptake rates in *Ditylum brightwellii*. Limnol. Oceanogr. **20:** 604–617.

PAINE, R. T. 1966. Food web complexity and species diversity. Am. Nat. **100:** 65–76.

PASCIAK, W. J., AND J. GAVIS. 1974. Transport limitation of nutrient uptake in phytoplankton. Limnol. Oceanogr. **19:** 881–888.

PETERSON, R. 1975. The paradox of the plankton: An equilibrium hypothesis. Am. Nat. **109:** 35–49.

REYNOLDS, W. C. 1989. Direct and large-eddy simulations of turbulence, p. 535. *In* J. Lumley [ed.], Whither turbulence? Springer-Verlag.

RICHERSON, P., R. ARMSTRONG, AND C. R. GOLDMAN. 1970. Contemporaneous disequilibrium, a new hypothesis to explain the "paradox of the plankton." Proc. Natl. Acad. Sci. USA **67:** 1719–1714.

RILEY, G. A., H. STOMMEL, AND D. F. BUMPUS. 1949. Quantitative ecology of the plankton of the western North Atlantic. Bull. Bingham Oceanogr. Collect. Yale Univ. **12:** 1–169.

ROTHSCHILD, B. J. 1991. Food signal theory: Population regulation and functional response. J. Plankton Res. **13:** 1123–1135.

———. 1992. Application of stochastic geometry to problems in plankton ecology. Philos. Trans. R. Soc. Lond. Ser. B Biol. Sci. **336:** 225–257.

———, AND T. R. OSBORN. 1988. Small-scale turbulence and plankton contact rates. J. Plankton Res. **10:** 465–474.

SARMIENTO, J. L., AND C. LEQUERE. 1996. Oceanic carbon dioxide uptake in a model of century-scale global warming. Science **274:** 1346–1350.

SIEGEL, D. A., AND J. A. DOMARADZKI. 1994. Large-eddy simulation of the decay of stably-stratified oceanic turbulence. J. Phys. Oceanogr. **24:** 2353–2386.

———, R. ITURRIAGA, R. R. BIDIGARE, H. PAK, R. C. SMITH, T. D. DICKEY, J. MARRA, AND K. S. BAKER. 1990. Meridional variations of the springtime phytoplankton community in the Sargasso Sea. J. Mar. Res. **48:** 379–412.

———, AND A. J. PLUEDDEMANN. 1991. The motion of a solid sphere in an oscillating flow: An evaluation of remotely-sensed Doppler velocity estimates in the sea. J. Atmos. Ocean. Technol. **8:** 296–304.

SOMMER, U. 1983. Nutrient competition between phytoplankton species in multispecies chemostat experiments. Arch. Hydrobiol. **96:** 399–416.

———. 1984. The paradox of the plankton: Fluctuations of the phosphorous availability maintain phytoplankton diversity in flow-through cultures. Limnol. Oceanogr. **29:** 633–636.

———. 1985. Comparison between steady-state and nonsteady state competition: Experiments with natural phytoplankton. Limnol. Oceanogr. **30:** 335–346.

———. 1988. Some size relationships in phytoflagellate motility. Hydrobiologia **161:** 125–131.

———. 1989. The role of competition for resources in phytoplankton succession, p. 57–106. *In* U. Sommer [ed.], Plankton ecology; succession in plankton communities. Springer-Verlag.

STEELE, J. H. 1974. The structure of marine ecosystems. Harvard Univ. Press.

SVERDRUP, H. U. 1953. On the conditions for the vernal blooming of phytoplankton. J. Cons. Cons. Perm. Int. Explor. Mer **18:** 287–295.

TENNEKES, H., AND J. L. LUMLEY. 1972. A first course in turbulence. MIT Press.

THOMAS, W. H., AND C. H. GIBSON. 1990. Quantified small-scale turbulence inhibits a red tide dinoflagellate, *Gonyaulax polyedra* Stein. Deep-Sea Res. **37:** 1583–1593.

TILMAN, D. 1977. Resource competition between planktonic algae: An experimental and theoretical approach. Ecology **58:** 338–348.

———. 1982. Resource competition and community structure. Princeton Univ. Press.

———, S. S. KILIIAM, AND P. KILIIAM. 1982. Phytoplankton com-

munity ecology: The role of limiting nutrients. Annu. Rev. Ecol. Syst. **13:** 349–372.

———, M. MATTSON, AND S. LANGER. 1981. Competition and nutrient kinetics along a temperature gradient: An experimental test of a mechanistic approach to niche theory. Limnol. Oceanogr. **26:** 1020–1033.

TRITTON, D. J. 1988. Physical fluid dynamics, 2nd ed. Oxford Scientific.

VOGEL, S. 1981. Life in moving fluids: The physical biology of flow. W. Grant.

YAMAZAKI, H., T. R. OSBORN, AND K. D. SQUIRES. 1991. Direct numerical simulation of planktonic contact in turbulent flow. J. Plankton Res. **13:** 629–643.

*Received: 16 October 1997*
*Accepted: 15 May 1998*
*Amended: 27 May 1998*